0026-895X/07/7104-1006–1014$20.00
MOLECULAR PHARMACOLOGY
Vol. 71, No. 4
32953/3188169
Mol Pharmacol 71:1006–1014, 2007
Printed in U.S.A.

Differential Selection of Acridine Resistance Mutations in Human DNA Topoisomerase IIβ Is Dependent on the Acridine Structure[S]

Chrysoula Leontiou,[1] Gary P. Watters, Kathryn L. Gilroy, Pauline Heslop, Ian G. Cowell, Kate Craig, Robert N. Lightowlers, Jeremy H. Lakey, and Caroline A. Austin

The Institute for Cell and Molecular Biosciences, the Medical School, Newcastle University, Newcastle upon Tyne, United Kingdom

Received November 28, 2006; accepted January 5, 2007

ABSTRACT

Type II DNA topoisomerases are targets of acridine drugs. Nine mutations conferring resistance to acridines were obtained by forced molecular evolution, using methyl *N*-(4′-(9-acridinylamino)-3-methoxy-phenyl) methane sulfonamide (mAMSA), methyl *N*-(4′-(9-acridinylamino)-2-methoxy-phenyl) carbamate hydrochloride (mAMCA), methyl *N*-(4′-(9-acridinylamino)-phenyl) carbamate hydrochloride (AMCA), and *N*-[2-(dimethylamino)ethyl]acridines-4-carboxamide (DACA) as selection agents. Mutations βH514Y, βE522K, βG550R, βA596T, βY606C, βR651C, and βD661N were in the B′ domain, and βG465D and βP732L were not. With AMCA, four mutations were selected (βE522K, βG550R, βA596T, and βD661N). Two mutations were selected with mAMCA (βY606C and βR651C) and two with mAMSA (βG465D and βP732L). It is interesting that there was no overlap between mutation selection with AMCA and mAMSA or mAMCA. AMCA lacks the methoxy substituent present in mAMCA and mAMSA, suggesting that this motif determines the mutations selected. With the fourth acridine DACA, five mutations were selected for resistance (βG465D, βH514Y, βG550R, βA596T, and βD661N). βG465D was selected with both DACA and mAMSA, and βG550R, βA596T, and βD661N were selected with both DACA and AMCA. DACA lacks the anilino motif of the other three drugs but retains the acridine ring motif. The overlap in selection with DACA and mAMSA or AMCA suggests that altered recognition of the acridine moiety may be involved in these mutations. We used restriction fragment length polymorphisms and heteroduplex analysis to demonstrate that some mutations were selected multiple times (βG465D, βE522K, βG550R, βA596T, and βD661N), whereas others were selected only once (βH514Y, βY606C, βR651C, and βP732L). Here, we compare the drug resistance profile of all nine mutations and report the biochemical characterization of three, βG550R, βY606C, and βD661N.

Type II DNA topoisomerases are ubiquitous enzymes essential for DNA transcription, DNA replication, and chromosome segregation. Topoisomerase II (topoII) passes one double helix through another via an ATP-dependent mechanism in which a "gate" DNA helix is covalently linked to the enzyme active-site tyrosine via a 5′-phosphate DNA linkage, cleaved, and a "transported" DNA helix is passed through the gap, which is subsequently resealed. The enzyme-DNA complex is termed the "cleavable complex," because addition of detergent to the normally transient intermediate results in cleaved DNA.

Type II topoisomerases are important targets for antibacterial and anticancer drugs. Poisons, which stabilize the normally transient cleavable complex and inhibit gate helix religation, are clinically the most widely used anti-topoII drugs, exerting cytotoxicity through the accumulation of DNA breaks, leading to apoptosis and cell death (Austin and Marsh, 1998). Atypical drug resistance toward poisons can occur via various mechanisms involving lower topoII protein expression or enzyme alterations through mutation. Muta-

This work was supported by Cancer Research UK (to C.L.) and the Wellcome Trust (to G.P.W.).
[1] Current affiliation: ETH Zürich, Institute for Molecular Biology and Biophysics, Zürich, Switzerland.
Article, publication date, and citation information can be found at http://molpharm.aspetjournals.org.
doi:10.1124/mol.106.032953.
[S] The online version of this article (available at http://molpharm.aspetjournals.org) contains supplemental material.

ABBREVIATIONS: topoII, topoisomerase II; mAMSA, amsacrine, methyl *N*-(4′-(9-acridinylamino)-3-methoxy-phenyl) methane sulfonamide; mAMCA, methyl *N*-(4′-(9-acridinylamino)-2-methoxy-phenyl) carbamate hydrochloride; AMCA, methyl *N*-(4′-(9-acridinylamino)-phenyl) carbamate hydrochloride; DACA, *N*-[2-(dimethylamino)ethyl]acridines-4-carboxamide; kDNA, kinetoplast DNA; MLC, minimum lethal concentration; bp, base pair(s); kb, kilobase(s); RFLP, restriction fragment length polymorphism; PCR, polymerase chain reaction; WT, wild type; ICRF-187, dexrazoxane.

tions can cause resistance by altering either drug interaction sites or steps in catalysis such that DNA binding and cleavage activities are impeded (Pommier, 1993).

Humans have two topoII isoforms, α and β, with distinct chromosomal locations. Both isoforms are up-regulated in G_2/M (Padget et al., 2000). TopoIIα is an important target and has sometimes been assumed to be the major cytotoxic target in vivo. The topoII poison etoposide seems to mainly target topoIIα in cultured cells (Willmore et al., 1998; Errington et al., 1999, 2004), but the relative effects on topoIIα and β in whole organisms are harder to determine. Murine cells lacking topoIIβ are significantly resistant to mAMSA, AMCA, and mAMCA, indicating that topoIIβ is also an important target for anticancer cytotoxicity and plays a role in drug action (Errington et al., 1999). In addition, human topoIIα and β cleave with mAMSA at similar cleavage sites (Marsh et al., 1996), and mAMSA-stabilized topoIIα and β cleavable complexes are equally stable in vitro.

One clinically relevant class of poisons is the acridines, in particular amsacrine (mAMSA), which is used in leukemia treatment (Jehn, 1989). mAMSA homologs AMCA and mAMCA are distinguished from mAMSA by their ability to target noncycling cells. Experiments in yeast showed that these drugs target α and β with similar affinity (Turnbull et al., 1999). Cleavage with AMCA is at sites distinct from those induced with mAMSA, with a similar pattern seen with both isoforms (Baguley et al., 1997). Some cellular responses to mAMCA differ from those to mAMSA (Moreland et al., 1997). DACA is an acridine that is reported to have the potential to overcome atypical drug resistance (Finlay et al., 1996).

Mutations in T4 bacteriophage topoII conferring resistance to mAMSA gave rise to cross-resistance to the structurally distinct poisons etoposide, ellipticine, and mitoxantrone, and a common drug binding site was proposed (Huff and Kreuzer, 1990). Random mutagenesis of yeast topoII and selection with mAMSA identified mutations in the conserved PLRGKMLN region, at Ala642, and C-terminal truncations (Wasserman and Wang, 1994). Similarly human topoIIα mAMSA-resistant mutations E571K and R486K were identified giving >25-fold and >100-fold resistance, respectively (Patel et al., 2000). Mutation R486K, in the B′ domain PLRGK motif, was identified independently in two amsacrine-resistant human leukemia cell lines (Hinds et al., 1991; Lee et al., 1992).

We have used forced molecular evolution to identify human topoIIβ mutations conferring resistance to acridines in vivo. Mutations were identified using DNA sequencing, restriction fragment length polymorphism (RFLP), and heteroduplex (WAVE) analysis. RFLP analysis has been used previously to screen quinolone-resistant *Escherichia coli* isolates for mutations in the GyrA QRDR region (Fisher et al., 1989) and ciprofloxacin-resistant *Streptococcus pneumoniae* isolates for mutations in the ParC and GyrA QRDR regions (Pan et al., 1996). To our knowledge, this is the first reported use of WAVE to identify topoII mutations. Four acridines were used in the selection, mAMSA, mAMCA, AMCA, and DACA, and nine different mutations were identified. Seven were found in the B′ domain of the enzyme (βH514Y, βE522K, βG550R, βA596T, βY606C, βR651C, and βD661N), with only two, βG465D and βP732L, outside this region. The characterization of mutations βG465D, βE522K, and βP732L has been reported elsewhere (Leontiou et al., 2004, 2006; Gilroy et al., 2006). This is the first report of the mutations obtained with DACA and mAMCA and of how the mutations obtained varied between the four acridines. This is also the first reported characterization of βG550R, βY606C, and βD661N.

Materials and Methods

Chemicals and Drugs

mAMSA was obtained from the National Cancer Institute (Bethesda, MD). AMCA and mAMCA were kindly supplied by Professor B. C. Baguley (Auckland Cancer Society Research Center, University of Auckland, Auckland, New Zealand). DACA was kindly supplied by Dr. P. Charlton (Xenova, Cambridge, UK). Etoposide, doxorubicin, and ellipticine were purchased from Sigma (Poole, Dorset, UK). DNA sequencing was carried out by Lark Technologies Inc. (Takeley, Essex, UK). Oligonucleotides were ordered from Invitrogen (Paisley, UK). Radiochemicals were purchased from Amersham Biosciences (Little Chalfont, Buckinghamshire, UK), and enzymes were from New England Biolabs (Hitchin, Hertfordshire, UK) or Promega (Southampton, UK). kDNA was purchased from TopoGEN (Columbus, OH).

Random Mutagenesis and Selection with Drugs

Plasmid YEphTOP2βKLM (Meczes et al., 1997) was subjected to random mutagenesis and selected for drug resistance as described previously (Leontiou et al., 2004). Four selection agents were used: mAMSA, mAMCA, AMCA, and DACA. A library of mutated plasmids was transformed into *Saccharomyces cerevisiae* strain JN394*top2-4*, which has a temperature-sensitive mutation that allows growth at 25°C (the permissive temperature) but not 35°C (the nonpermissive temperature). Yeast growth at the nonpermissive temperature is dependent on functional plasmid-borne topoII. The transformants were selected for drug resistance by exposure to either 74.7 μg/ml mAMSA, 16.4 μg/ml mAMCA, 76 μg/ml AMCA, or 0.5 mg/ml DACA for 96 h in liquid culture at 35°C. Figure 1 shows the chemical structures of all four acridines used. Yeast were then grown on selective media lacking uracil and drug at the concentrations above for 3 to 5 days at 35°C. Colonies were then regrown on plates containing selecting drug to confirm resistance. From these clones, plasmids were rescued, and the possibility of gross rearrangements or deletions eliminated by analysis of restriction digestion patterns. Selected plasmids were then retransformed into yeast to verify that resistance was plasmid borne, and mutations were identified by sequencing both strands. The full coding sequence was

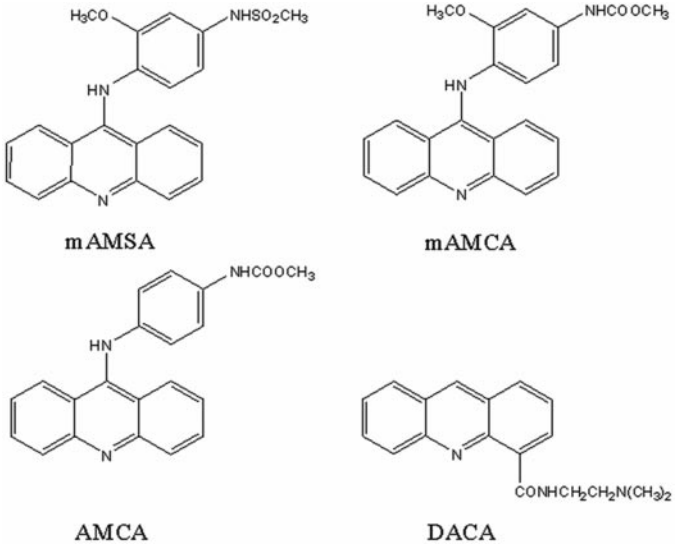

Fig. 1. Chemical structures of the four acridine drugs used in the study.

sequenced in the case of DACA, AMCA, and mAMSA. Figure 2 shows a flow diagram depicting the selection procedure.

Identification of Mutants by RFLP and WAVE

Because of the large number of resistant yeast isolated, it was not possible to retransform all plasmids into JN394t2-4. Plasmids not retransformed were screened for mutations identified by sequencing using RFLP and heteroduplex (WAVE) analysis.

RFLP analysis is based on alterations in the DNA sequence caused by a mutation leading to the loss or gain of a target site for a restriction enzyme. For this analysis, an approximately 1-kb region from bases 1083 to 2194, spanning the region containing mutations βG465D, βA596T, βY606C, βR651C, and βD661N, was amplified by PCR. Fragments were then digested with the relevant restriction enzyme (New England Biolabs) in recommended conditions and at the recommended temperature specified by the suppliers for at least 1 h. Table 1 shows the base changes and restriction enzymes for detection of each mutation. Reaction products were then separated on a 0.8% or 1% agarose/1× Tris borate-EDTA gel, stained with ethidium bromide, and visualized under UV light, and the gain or loss of a band as appropriate was noted.

For heteroduplex analysis, WAVE apparatus consisting of a DH-PLC machine with an HT column (Transgenomic, Crewe, Cheshire, UK), as has been described previously (Wulfert et al., 2006), was used. A 198-bp region, from 1501 to 1699, spanning target mutations βH514Y, βE522K, and βG550R was amplified by PCR in wild-type and sample plasmids. The primers used were: forward, 1501-CCA CTC AGG GGC AAA ATT C-1519; reverse, 1699-C TTT TAT GTG AGA ACC ATC-1681.

The melting profile of this region was determined by entering the sequence into Wavemaker software (Transgenomic); the ideal melting temperature was calculated, and a method was created for product elution using a suitable chemical gradient for this DNA sequence. Wild-type and unknown sample strands were mixed in a 1:1 ratio, melted at 95°C for 5 min, and then reannealed by cooling at room temperature to create a mixture of homodimers and heterodimers.

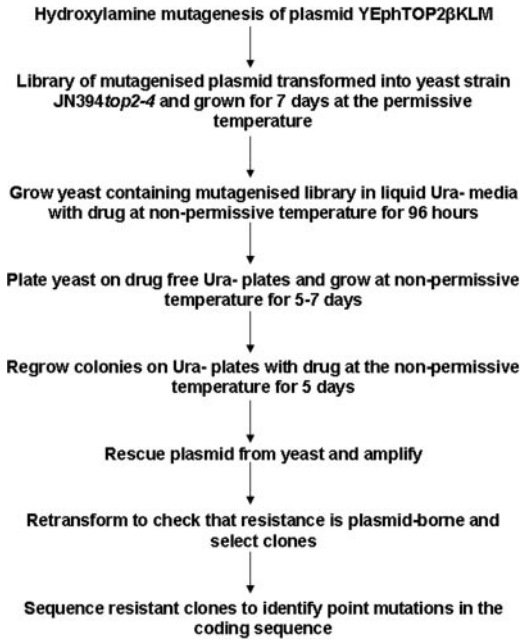

Fig. 2. Flow diagram showing the selection procedure of drug-resistant mutations. The permissive temperature is 25°C, and the nonpermissive temperature is 35°C. Drug concentrations in liquid culture were 500 μg/ml DACA, 76 μg/ml AMCA, 74.7 μg/ml mAMSA, and 16.4 μg/ml mAMCA. Drug concentration for selection on plates was the same as for liquid culture with the exception of 10 μg/ml mAMSA and 1 μg/ml mAMCA.

A standard volume of 5 μl was injected under partially denaturing conditions, and duplexes were eluted along the calculated gradient of buffer A (0.1 M triethylammonium acetate, pH 7) and buffer B (0.1 M triethylammonium acetate, 25% acetonitrile) as determined by the Wavemaker software. Increasing acetonitrile concentrations cause duplex elution from the column, with heteroduplexes eluting first because of the lower affinity of the mismatched sequences for the column, and then homoduplexes. An extra peak or "shoulder" from the homoduplex peak denotes the presence of a heteroduplex and, hence, a mutation. Subsequent DNA sequencing confirmed the identity of the mutation.

In Vivo Characterization

Rapid analysis of cross-resistance to a variety of drugs was determined by continuous exposure on agar plates containing the drug to be tested. Yeast cultures of known optical density were replica-plated and grown for 3 to 5 days at 35°C. Levels of resistance were determined from WT and mutant growth at different concentrations of drug (Leontiou et al., 2004). Resistance to mAMSA was further quantified by measuring the minimum lethal concentration (MLC) for wild-type and mutant topoIIβ. To ensure that resistance in the MLC assay was due to the point mutation and not other plasmid changes, fragment exchange of a 1674-bp fragment between sites BamHI and PmaCI containing all mutations into an unmutagenized plasmid was performed, and the presence of mutation was confirmed by DNA sequencing. Yeast were exposed to drug in liquid culture for 6 or 24 h and then grown on drug-free plates to determine the MLC as described previously (Leontiou et al., 2004).

In Vitro Characterization

Protein Production. Recombinant wild-type and mutant topoIIβ proteins were expressed in yeast strain Jel1Δtop1 bearing plasmid YEphTOP2βKLM, YEphTOP2βG550R, YEphTOP2βY606C, or YEphTOP2βD661N. These plasmids had been fragment-exchanged as described above. Protein purification was as described previously (Austin et al., 1995).

Strand Passage Assays. Decatenation and relaxation assays were carried out in "relaxation buffer" (50 mM Tris-HCl, pH 7.5, 0.5 mM EDTA, 1 mM dithiothreitol, 100 mM KCl, and 30 μg/ml bovine serum albumin), plus 2 mM ATP, 10 mM $MgCl_2$, and either 1 μg of supercoiled pBR322 plasmid DNA (for relaxation assays) or 400 ng of kinetoplast DNA (kDNA, for decatenation assays). The method used was as described previously (Austin et al., 1995; West et al., 2000).

DNA Cleavage Assays. Cleavage assays using a 40-bp oligonucleotide and a 4.3-kb linearized pBR322 plasmid were carried out as described previously (Marsh et al., 1996).

Surface Plasmon Resonance. Analysis of mutated protein binding to 40-bp immobilized biotinylated oligonucleotides, four-way junction, and bent DNA was carried out as described previously on a Biacore 2000 (Biacore, St. Albans, Hertfordshire, UK) (Leontiou et al., 2003, 2006).

Results

Selection with Drugs and Identification of Mutations. We used a forced molecular evolution approach to

TABLE 1
Mutations for which RFLP analysis was possible
The bases changed in mutation are underlined. The appropriate restriction enzyme and whether this leads to a gain or loss of site are shown.

Mutation	Codon Change	Enzyme	Gain/Loss
βG465D	GGT-GAT	HphI	Gain
βA596T	GCA-ACA	Cac8I	Loss
βY606C	TAC-TGC	PstI	Gain
βR651C	CGC-TGC	BsrDI	Gain
βD661N	GAT-AAT	Eco57I	Gain

generate and select mutations in human topoisomerase IIβ that confer resistance to the acridines mAMSA, mAMCA, AMCA, and DACA. The selection procedure is dependent on having a functional topoisomerase II protein produced from a plasmid. In each case, a selection of the colonies originally identified had plasmids rescued and were retransformed into JN394*top2-4* to verify that resistance was plasmid-borne. The plasmids conferring resistance were sequenced on both strands of the topoIIβ coding sequence.

After selection with DACA, 49 clones that grew on 500 μg/ml DACA were characterized further. After plasmid rescue and retransformation, 23 showed plasmid-borne resistance, and the topoIIβ coding region was sequenced. Five different mutations were identified in the coding sequence. A G-to-A change at position 1648 resulting in mutation βG550R was identified three times with DACA; a G-to-A change at position 1981, giving mutation βD661N, was identified once with DACA; a G-to-A change at 1786, giving mutation βA596T, was identified once with DACA; a G-to-A change at 1395, giving mutation βG465D, was identified once with DACA; and a C-to-T change at residue 1542, giving mutation βH514Y, was identified once with DACA. Sixteen plasmids showed no mutation in the coding sequence. The remaining plasmids were analyzed with RFLP and heteroduplex analysis (WAVE) methods as described under *Materials and Methods*, but no further replicates of the known mutations were identified. Mutations βG465D, βA596T, and βD661N all give rise to RFLPs (Table 1). For βG550R and βH514Y, for which RFLPs were not available, heteroduplex analysis was carried out.

Illustrative data for RFLP and WAVE are shown in Fig. 3. Figure 3A shows the identification of a βA596T mutant after digestion with Cac8I. Lane 1 shows the mutation, and lane 2 is a wild-type restriction pattern. Figure 3B shows a WAVE trace generated for a mixture of wild-type and βG550R mutant PCR products, and the arrow points to the additional heteroduplex peak "shoulder" on the homoduplex peak.

AMCA selection gave 48 clones on drug plates containing 76 μg/ml AMCA, and of these, 11 plasmids were transformed and sequenced. Overlap with DACA selection was seen with mutation βG550R identified four more times, βD661N identified three more times, and βA596T identified once more. In addition a G-to-A change at position 1564 giving mutation βE522K was identified once (reported in Leontiou et al., 2004). Two clones showed no mutation on sequencing the whole insert. RFLP analysis of all remaining plasmids from the AMCA pool revealed a further four βA596T mutations and a further five βD661N mutations, and WAVE identified one more βE522K mutation and five more βG550R mutations selected with AMCA.

In the mAMSA screen, 36 clones able to grow on plates containing 10 μg/ml mAMSA were identified, and three were identified as conferring resistance after retransforming into yeast. Overlap with DACA selection was seen, with mutation βG465D being selected twice more. In addition, a C-to-T change at position 2195, giving βP732L, was identified. RFLP analysis of all 36 plasmids identified a further βG465D mutation from the mAMSA pool, no further mutants were identified in this pool by WAVE analysis.

In the mAMCA screen, eight colonies were selected on plates containing 1 μg/ml mAMCA and were retransformed and sequenced. Of these eight, four were sequenced across the entire coding region, identifying one A-to-G change at position 1817, giving mutation βY606C, and one C-to-T change at position 1953, giving mutation βR651C. In the remaining four clones, the nine mutations identified previously were screened for by either sequencing the region spanning all known mutations, 1083 and 2250 bp, and by RFLPs. No mutations at positions selected with mAMSA, AMCA, or DACA were identified. Table 2 shows a summary of all of the mutations identified with each drug by DNA sequencing and indicates both total numbers and additional replicates selected with the RFLP and WAVE methods.

Cross-Resistance to Poisons Conferred by Mutations. The drug-resistance profile of each mutation to the acridines mAMSA, AMCA, mAMCA, DACA, the epipodophyllotoxin etoposide, the anthracycline doxorubicin, and ellipticine was measured by comparing growth of yeast carrying a plasmid encoding mutant enzyme with that encoding wild-type topoIIβ. These drugs represent a variety of structural classes of topoII poison. Equal amounts of yeast, as

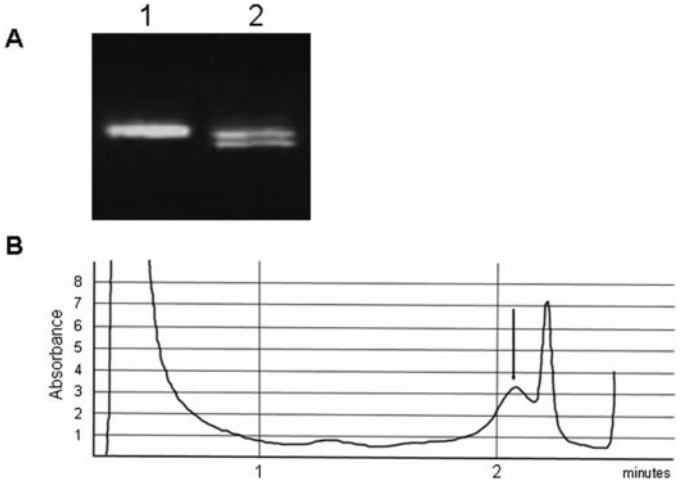

Fig. 3. Example of detection of a βA596T mutation after digestion of PCR fragments from sample plasmids with restriction enzyme Cac8I. A, lane 1 shows a single band denoting the loss of a Cac8I site with mutation. Lane 2 shows the wild-type restriction pattern giving two bands. B, example DHPLC elution trace seen with heteroduplex analysis (WAVE) showing the presence of mutation βG550R. The peak indicated by the arrow denotes the presence of a heteroduplex that elutes before the other, homoduplex peak.

TABLE 2
A summary of which mutations were found with which selection agent and the base change and position of mutation
The total number of selections is shown, with values in parentheses showing the selections of these with either RFLP (for βG465D, βA596T, and βD661N) or WAVE (for βE522K and βG550R).

Mutation	Base Change	Position	Selection	No. of Times Selected
βG465D	G→A	1395	mAMSA	3 (1)
			DACA	1
βH514Y	C→T	1542	DACA	1
βE522K	G→A	1564	AMCA	2 (1)
βG550R	G→A	1648	AMCA	9 (5)
			DACA	3
βA596T	G→A	1786	AMCA	5 (4)
			DACA	1
βY606C	A→G	1817	mAMCA	1
βR651C	C→T	1953	mAMCA	1
βD661N	G→A	1981	AMCA	8 (5)
			DACA	1
βP732L	C→T	2195	mAMSA	1

determined by optical density, were plated onto adenine-supplemented yeast extract/peptone/dextrose plates supplemented with increasing concentrations of drug and were grown for 5 days at the nonpermissive temperature. A summary of the approximate -fold resistances or hypersensitivity conferred by each mutation to each drug is shown in Table 3, with the selecting agents shown in boldface type. Full-growth profiles with each mutation for increasing concentrations of drug are shown in Supplemental Table S1.

In most cases, the mutations confer resistance to the selection agent and cross-reactivity to multiple antitopoisomerase drugs (Table 3). But in the drug plate assays, βY606C shows wild-type sensitivity levels, and for βR651C, which seems slightly hypersensitive to mAMCA, in these cases low-level resistance cannot be excluded, because growth on plates containing the selecting drug for 5 days does not always parallel the results seen in experiments in which yeast are exposed to drug in liquid culture. For example, βG465D showed a statistically significant 10-fold resistance after exposure to mAMSA for 6 h in a quantitative MLC assay, in which the yeast transformants were exposed to mAMSA in liquid culture for 6 h followed by growth in drug-free plates, yet on continuous exposure to drug on plates for 5 days, yeast transformed with the βG465D mutation grew at a rate comparable with wild-type yeast; this has been reported elsewhere, and a mechanism for this differential effect is suggested (Gilroy et al., 2006). All mutations confer resistance to DACA and ellipticine with the exception of βE522K, which has been reported previously (Leontiou et al., 2004). Mutations βA596T, βD661N, and βP732L show resistance to all acridines, whereas all others show some wild-type sensitivity or hypersensitivity to differing acridines.

Mutations βH514Y, βA596T, and βR651C, although interesting, were not characterized further. Mutations βG465D, βE522K, and βP732L have been described previously (Leontiou et al., 2004, 2006; Gilroy et al., 2006). In this manuscript, we focus on βD661N, βG550R, and βY606C and compare these with the other six mutations.

Resistance to mAMSA Conferred by Mutations. Drug resistance to mAMSA was measured quantitatively using the minimum lethal concentration method (Nitiss, 1994). JN394*top2-4* transformed with plasmid encoding either wild type, βD661N, βY606C, or βG550R topoIIβ was grown in the presence of increasing concentrations of mAMSA for 6 or 24 h, and then the amount of growth relative to a t_0 plate was quantified for all yeast strains. Results are the average of at least three independent experiments.

Wild-type MLC values were 1.5 and 2.5 μg/ml at 6 and 24 h, respectively. In this assay, the mutations βG550R, βY606C, or βD661N did not confer significant resistance to mAMSA, as determined by a two-tailed, paired Student's *t* test. MLC values for βG550R were 4 and 1.25 μg/ml, for βY606C were 6.25 and 2.5 μg/ml, and for βD661N were 1.7 and 3.1 μg/ml, at 6 and 24 h, respectively. In contrast, the MLC values for βE522K, βP732L, and βG465D on mAMSA were statistically significant in most cases as has been reported elsewhere (Leontiou et al., 2004, 2006; Gilroy et al., 2006). To allow comparison, the MLCs when exposed to mAMSA are 20 and >20 μg/ml for βE522K, 14.8 and 24.8 μg/ml for βP732L, and 10 and 5 μg/ml for βG465D.

Cleavage of a 40-bp Oligonucleotide. Cleavage by mutants βG550R, βY606C, and βD661N were compared with wild type using a 40-bp oligonucleotide as described under *Materials and Methods*. This oligonucleotide contains an

TABLE 3

Summary of cross-resistance conferred by each mutation to a range of drugs

-Fold resistance relative to wild-type sensitivity is shown unless hypersensitivity is described. WT indicates no change in sensitivity relative to wild type. Values in bold are the selection agents for each mutation.

Plasmid	Resistance Factor to Drug						
	mAMSA	mAMCA	AMCA	DACA	Etoposide	Doxorubicin	Ellipticine
YEphtop2βG465D	**WT**	~5-fold	~2-fold	~**20-fold**	~4-fold	~2-fold	~10-fold
YEphtop2βH514Y	~2-fold sensitive	~5-fold sensitive	WT	~**5-fold**	~2-fold sensitive	WT	~4-fold
YEphtop2βE522K	~10-fold	~10-fold	~**5-fold**	~10-fold sensitive	~10-fold sensitive	~2-fold	~5-fold sensitive
YEphtop2βG550R	WT	~2-fold	~**5-fold**	~**20-fold**	~4-fold	~2-fold	~10-fold
YEphtop2βA596T	~2.5-fold	~5-fold	~**5-fold**	~**20-fold**	~2-fold	WT	~20-fold
YEphtop2βY606C	~2-fold sensitive	**WT**	~5-fold	~20-fold	~2-fold	~2-fold	~10-fold
YEphtop2βR651C	~5-fold sensitive	**WT**	WT	~10-fold	WT	~2-fold	~4-fold
YEphtop2βD661N	~5-fold	~5-fold	~**5-fold**	~**20-fold**	~2-fold	~2-fold	~20-fold
YEphtop2βP732L	~**10-fold**	~50-fold	~50-fold	~20-fold	~4-fold	~5-fold	~20-fold

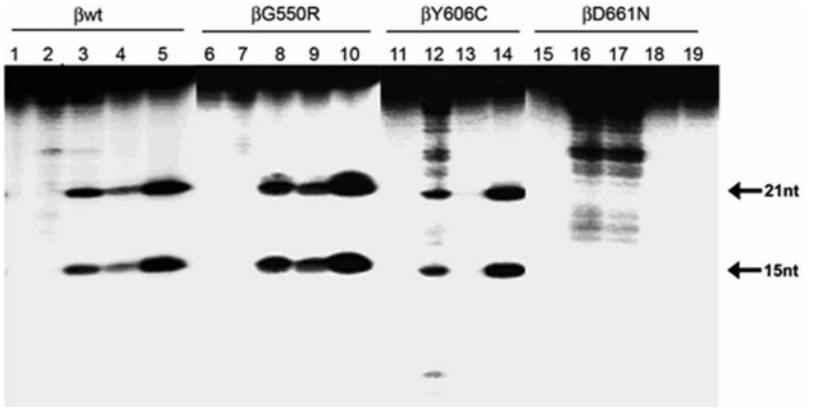

Fig. 4. Cleavage of a 40-bp oligonucleotide giving two product bands at sizes 21 and 15 nucleotides. Proteins βWT (lanes 1–5), βG550R (lanes 6–10), βY606C (lanes 11–14), and βD661N (lanes 15–19) are shown. No protein controls are seen in lanes 1, 6, and 15; cleavage in the presence of 10 mM $MgCl_2$ in lanes 2, 7, 11, and 16; cleavage in the presence of 10 mM $MgCl_2$ and 10 μg/ml mAMSA in lanes 3, 8, 12, and 17; cleavage in presence of 10 mM $CaCl_2$ in lanes 4, 9, 13, and 18; cleavage in the presence of 10 mM $CaCl_2$ and 10 μg/ml mAMSA in lanes 5, 10, 14, and 19. Image is representative of three independent experiments.

mAMSA site that is cleaved strongly in the presence of mAMSA and weakly in its absence to give two products of 21 and 15 base pairs (Marsh et al., 1996). Cleavage was measured with 10 mM $MgCl_2$ or $CaCl_2$ in the presence or absence of 10 μg/ml mAMSA. Results are shown in Fig. 4. Wild-type cleavage with magnesium was enhanced by the addition of mAMSA, increasing from 7.8 ± 2.4 to 100%, respectively. Calcium promotes more cleavage with wild type than magnesium at 42 ± 7.7, and calcium cleavage is also enhanced by mAMSA to 376.4 ± 97.6, taking 100% to be wild-type cleavage with magnesium and mAMSA.

βG550R consistently showed approximately double wild-type levels of cleavage, with magnesium-stimulated cleavage of 248.7 ± 13.9 and 18.9 ± 6.1 in the presence or absence of mAMSA, respectively, and calcium-stimulated cleavage of 689.4 ± 136.8 and 93.5 ± 65.9 in the presence or absence of mAMSA, respectively. Because of large standard deviations, however, only the βG550R cleavage with magnesium and mAMSA was statistically significant with $p > 0.01$ as determined by two-tailed Student's t test.

βY606C showed slightly reduced cleavage with values with magnesium of 48.8 ± 28.8 and 6.2 ± 1.5 in the presence and absence of mAMSA, respectively. These differences were not statistically significant. With magnesium, in addition to the expected 15 and 21 nucleotide bands, there were multiple other bands seen. With calcium βY606C also showed reduced cleavage with values of 181.2 ± 95 and 6.6 ± 4.4 in the presence or absence of mAMSA, respectively. Whereas cleavage with calcium and mAMSA was not significantly different from wild type, cleavage with calcium alone was statistically significantly lower than wild type, with $p > 0.01$ in a two-tailed t test.

The pattern of cleavage for βD661N with magnesium is distinct from wild type with multiple bands present, and the 15 and 21 nucleotide bands were not seen, so it was not possible to quantify in a comparable way with wild type. With calcium, βD661N cleavage was significantly reduced in the presence and absence of mAMSA with values of 6 ± 2.3 ($p < 0.05$) and 2.9 ± 1.4 ($p < 0.01$), respectively.

Wild-type topoIIβ is able to cleave the 40-bp oligonucleotide in the presence of 100 μg/ml etoposide and 10 mM $MgCl_2$. Taking wild-type cleavage as 100%, mutant cleavage was determined and compared with this. βY606C showed cleavage levels similar to wild type with etoposide at 87.9% ± 4.7, as did βG550R at 114.2% ± 13.5, in contrast to mAMSA cleavage, which was increased. βD661N showed the least cleavage with etoposide at 73.2% ± 5.6.

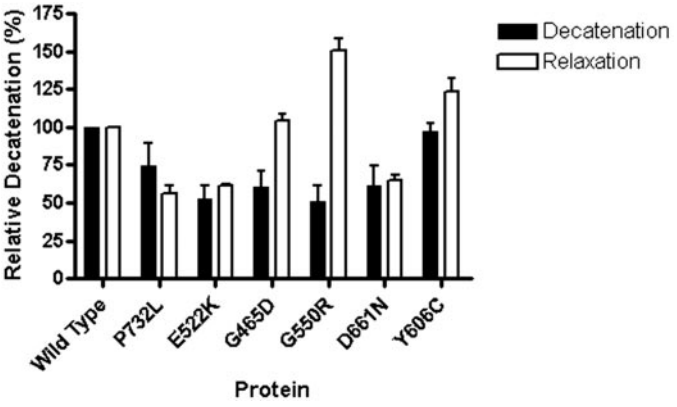

Fig. 5. Strand passage activity of mutants. Decatenation is shown as black bars and relaxation as white bars. Mutant activity is calculated relative to wild type, taken as 100%. Error bars representing one standard deviation from the mean are shown. Data are the average of at least three independent experiments.

Strand Passage. Decatenation and relaxation assays were carried out with wild-type, βD661N, βY606C, and βG550R topoIIβ proteins as described under *Materials and Methods*. Wild-type values are taken as 100% with mutant activity relative to this, and a minimum of three experiments were averaged. Data are shown in Fig. 5 along with previously reported mutations βG465D, βE522K, and βP732L for comparison. βY606C shows no significant difference from wild type in either relaxation or decatenation assays, with values of 123.7 ± 15.6 and 97 ± 8.9, respectively. βD661N shows reduced decatenation at 61.3% ± 23.3, and this difference is not statistically significant. βD661N shows significantly less relaxation at 65.1% ± 5.3 ($p < 0.01$). βG550R shows significantly more relaxation at 150% ± 17.1 ($p < 0.01$), and significantly less decatenation at 50.6% ± 18.5 ($p < 0.05$). Significance in all cases was determined using a two-tailed Student's t test.

DNA Binding Properties. Results of DNA binding experiments for each mutated protein using surface plasmon resonance are summarized in Table 4 with full figures in Supplemental Table S2. Dissociation constants for each mutated protein are shown for three different DNA substrates: 40-bp oligonucleotide, four-way junction oligonucleotide, or bent DNA. Wild-type K_D values are shown for comparison and have been described previously (Leontiou et al., 2003). Mutation βG550R shows reduced DNA binding to the 40-bp oligonucleotide, although binding to the four-way junction and bent substrates is similar to that of wild type. Both βD661N and βY606C bound to all three substrates with an apparently lower affinity than wild type, but the differences were not statistically significant.

ATP and Magnesium Dependence. The effect of increasing ATP concentration on decatenation activity was measured for each mutant compared with wild type. None of the mutations tested, βG550R, βY606C, or βD661N, showed any significant difference from wild type (data not shown). The effect of increasing magnesium on decatenation was also measured. Both βD661N and βY606C showed a magnesium

TABLE 4
Summary of Biacore binding data of wild-type and mutant topoIIβ to three different DNA substrates
Experimental values K_a and K_d are used to calculate the K_A and K_D for the reaction. The K_D value for wild type is shown for comparison and has been reported previously (Leontiou et al, 2003).

Protein and DNA Substrate	K_a	K_d	K_A	K_D	Wild-Type K_D
	$M^{-1}S^{-1} \times 10^6$	$S^{-1} \times 10^{-3}$	$M^{-1} \times 10^8$	$M \times 10^{-9}$	$M \times 10^{-9}$
βD661N					
40 bp	0.80 ± 0.42	2.22 ± 0.37	3.60	2.78	1.73
4 wj	0.59 ± 0.02	1.51 ± 0.41	3.91	2.56	2.85
Bent	0.43 ± 0.21	1.58 ± 0.24	2.72	3.67	1.86
βY606C					
40 bp	0.79 ± 0.49	2.11 ± 0.06	3.74	2.67	1.73
4 wj	0.56 ± 0.26	1.52 ± 0.07	3.68	2.71	2.85
Bent	0.35 ± 0.26	1.53 ± 0.06	2.29	4.37	1.86
βG550R					
40 bp	0.58 ± 0.18	3.15 ± 0.53	1.84	5.43	1.73
4 wj	0.43 ± 0.28	1.54 ± 0.31	2.79	3.58	2.85
Bent	0.25 ± 0.19	1.45 ± 0.26	1.72	5.80	1.86

4 wj, four-way junction.

optima similar to that of wild type, with maximal decatenation activity between 10 and 30 mM $MgCl_2$, 80% at 40 mM, and approximately 50% at 50 mM $MgCl_2$. Mutation βG550R showed a narrower magnesium optima than wild type, with a substantial reduction in decatenation activity at higher magnesium concentrations. Between 30 and 50 mM $MgCl_2$ βG550R showed approximately 20% activity (Fig. 6).

Discussion

We have selected mutations in human topoisomerase IIβ that confer resistance to the acridines mAMSA, mAMCA, AMCA, and DACA (Fig. 7). The selection process will only select functional enzymes. We report for the first time the selection of mutations in topoisomerase IIβ with DACA and mAMCA. We used heteroduplex and RFLP analysis to locate mutations in topoisomerases.

Different mutation profiles were selected with each of the four acridines, suggesting that there is discrimination in the action of these drugs. AMCA selects different mutations to mAMCA and mAMSA. Two mutations, βG465D and βP732L, were selected with mAMSA and two, βY606C and βR651C, with mAMCA.

With DACA, five mutations were selected, and with AMCA four; three mutations (βG550R, βD661N, and βA596T) were selected multiple times with either DACA or AMCA. βG550R, βD661N, and βA596T were selected a total of 12, 9, and 6 times, respectively (Table 2). DACA also showed overlap with mAMSA in one case, selecting βG465D, which may suggest less specific selection with this drug. An overlap in the selection with AMCA with DACA as opposed to mAMCA and mAMSA is unexpected because structurally, AMCA is more similar to mAMCA and mAMSA with all three having an anilino motif that DACA lacks (Fig. 1).

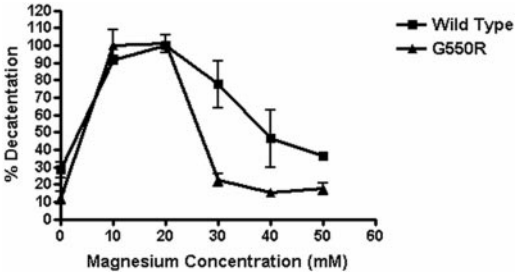

Fig. 6. Dependence of decatenation of β wild type (■) and βG550R (▲) on magnesium concentration. The highest decatenation seen with each protein was taken as 100%, and all other values were calculated relative to this. Error bars represent one standard deviation from the mean. The average of two independent experiments is shown.

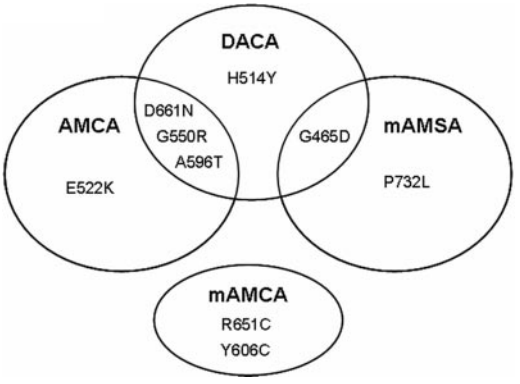

Fig. 7. Venn diagram showing selection of mutations with AMCA, DACA, mAMSA, and mAMCA. Overlap of selection with DACA with selection with either mAMSA or AMCA is shown.

All four drugs share the acridine ring system, so the commonality of this in AMCA and DACA is not a satisfactory explanation. All that distinguishes AMCA from both mAMCA and mAMSA is the presence of a methoxy substituent on the anilino ring, implying that the presence of this disfavors selection of βG550R, βA596T, and βD661N. It has been hypothesized previously that drugs bind to a pocket consisting of both enzyme and DNA in a complex and that specific drugs have different preferences (Huff and Kreuzer, 1990; Baguley et al., 1997). In addition, the mAMSA anilino motif has been implicated in interaction with the drug binding site's protein element and the acridine ring system with the DNA through intercalation (Capranico et al., 1998). It seems likely that AMCA forms a ternary complex with unique DNA and enzyme interactions that favor the selection of the mutations above. Indeed, previously, AMCA has been shown to cleave at sites distinct from mAMSA, implying differences in the ternary complex (Baguley et al., 1997). The reason for the higher number of mutations identified with AMCA is unclear but may be related to the stability of the ternary complex with these mutations or the in vivo activity conferred by them.

The nine mutations confer different cross-resistance patterns to poisons, implying that there is more than one resistance mechanism. βG465D was selected four times, once with DACA and three times with mAMSA. We hypothesized previously that this impedes signal transduction through conformational changes from the cleavage-religation core domain to the N-terminal ATPase domain and thus slows enzyme turnover, causing drug resistance (Gilroy et al., 2006). mAMSA alone selected βP732L, which has high levels of resistance to all drugs. Here, we hypothesized that local conformational changes might alter the ligand geometry for metal ions involved in catalysis, altering phosphoryl transfer (Leontiou et al., 2006). All mutations conferred resistance to DACA and ellipticine except βE522K, selected with AMCA, which is hypersensitive to both of these agents and to etoposide. The hypersensitivity to etoposide has been discussed previously (Leontiou et al., 2004). We hypothesized that βE522 coordinates a structural metal ion, and mutation to lysine alters a drug-binding pocket, giving differential effects with different drugs (Leontiou et al., 2004). It is interesting to note that βH514Y, in the same region as βE522K, is also resistant to some drugs but hypersensitive to others, suggesting that H514Y may alter the drug-binding pocket affected by βE522K. βY606C and βR651C were selected with mAMCA, but neither confers resistance to mAMCA upon continuous exposure. βY606C confers moderate resistance to AMCA, etoposide, doxorubicin, and ellipticine, with no alteration in strand passage, ATP-dependence, magnesium optima, or DNA binding; however, cleavage of a 40-bp oligonucleotide was reduced significantly with calcium. Because of time constraints, βH514Y, βA596T, and βR651C were not pursued.

Mutation βG550R was selected 12 times, 9 times with AMCA and 3 with DACA. It shows increased cleavage and significantly increased relaxation, but it was surprising that its decatenation activity is significantly reduced. An alteration in the cleavage-religation equilibrium of this enzyme,

causing acceleration of the forward reaction (cleavage) and/or inhibition of the reverse reaction (religation), could account for this phenotype. Decatenation and relaxation assays are not equivalent in that relaxation is intramolecular (once on the DNA, topoIIβ acts continuously to generate a ladder of products), and decatenation of kDNA is intermolecular (once a pair of minicircles has been decatenated, the enzyme must move through the catalytic cycle to capture another catenated minicircle). If the reverse reaction of the βG550R mutant is impeded such that resealing a DNA break and moving onto another substrate molecule is slowed, reduced decatenation and increased relaxation would be predicted.

βG550R cleavage is enhanced by mAMSA but not by etoposide with the 40-bp oligonucleotide, and the magnesium optima is narrowed, as was seen with βG465D and βP732L (Gilroy et al., 2006; Leontiou et al., 2006). In the topoIIβ structure modeled on yeast topoII (Protein Database code 1BGW), residue βGly550 is 11 Å from residue βGly465. However, βG465D showed phenotypic differences from βG550R in that βG465D had a 3-fold increase in ATP requirement, not seen with βG550R, so it seems unlikely that a similar mechanism is taking place (Gilroy et al., 2006). A triad of aspartate residues, βAsp557, βAsp559, and βAsp561, in the conserved IMTDQDXD (554–561) region of topoIIβ is proposed to form a cation binding site that moves to interact with the catalytic site during cleavage (West et al., 2000; Noble and Maxwell, 2002). βGly550 lies between 21 and 28 Å from these aspartate residues (Fig. 8), and in the primary sequence, it is very close to βAsp557, βAsp559, and βAsp561. Thus, it is possible that the altered magnesium optima could be caused by alteration of the cation binding site, and thus magnesium coordination, by the G550R mutation. The coordination of magnesium by aspartates is proposed to be intricately involved in the cleavage mechanism of DNA topoisomerases and DNA polymerases, stabilizing the active site tyrosine before nucleophilic attack on the DNA phosphate (Beese and Steitz, 1991; Noble and Maxwell, 2002). An alteration in the cation binding site could therefore affect cleavage. The proposed topoIIβ drug binding site consists of protein and bound DNA, with drugs preferring specific DNA sequences (Baguley et al., 1997; Capranico et al., 1998). Cleavable complexes are therefore to an extent drug-specific, with different poisons giving different arrangements, which could account for the enhanced cleavage seen with mAMSA but not etoposide.

βD661N cleavage of the 40-bp oligonucleotide with magnesium gave a different pattern of bands from wild type, with multiple bands seen instead of the expected 15 and 21 nucleotide bands. Mutation βD661N has vastly reduced cleavage of a 40-bp oligonucleotide with calcium. The residue βAsp661 lies in the disordered region of the yeast structure but is adjacent to the last ordered residue, so its rough position can be estimated (Fig. 8). βAsp661 lies approximately 12 Å from the active site tyrosine. The model structure used is just a snapshot of one position in a dynamic molecule, and so considerable movement during the catalytic cycle is expected. However, it remains a distinct possibility that the reversal of charge from aspartate to asparagine in βD661N could affect key interactions necessary for DNA cleavage. The βD661N mutation may cause local conformational changes that disfavor the coordination of calcium, meaning it cannot support the phosphoryl transfer reaction during cleavage. On the other hand, the lack of cleavage with calcium could be explained by the acidic residues in the loop adjacent to βAsp661 (residues βAsp662, βAsp675, βAsp676, βGlu679, βGlu686, and βAsp687) coordinating a structural metal ion, and this coordination is affected by mutation. Unfortunately, these residues lie in a disordered region and cannot be modeled. The mutation equivalent to βD661N in human topoIIα, αD654N, was selected previously for resistance to ICRF-187, and it was suggested that resistance may be due to either altered stability of the closed clamp or reduced enzymatic activity, the latter of which is consistent with our results (Jensen et al., 2000). αD654N has no cross-resistance to etoposide or mAMSA, unlike βD661N, which has 2- and 5-fold cross-resistance to etoposide and mAMSA, respectively, possibly indicating slight differences between the two isoforms. The reduced decatenation seen with αD654N is consistent with that seen with βD661N.

We selected nine mutations with differing phenotypes in a forced molecular evolution screen selecting with acridines. As expected, the mutations seemed to fall into two broad categories, those affecting drug binding (βE522K, βH514Y), and

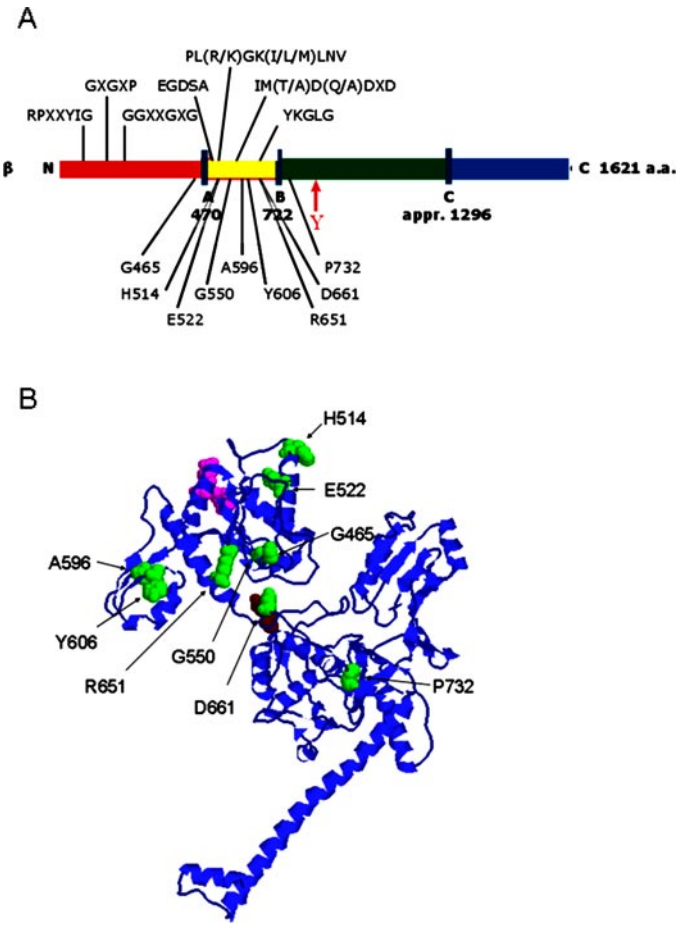

Fig. 8. A, figure adapted from Austin and Marsh, 1998, showing the domains of human topoisomerase IIβ; in red is the N-terminal ATP hydrolysis domain, in yellow is the B′ domain, in green the A′ subdomain, and in blue the C-terminal domain. Together the A′ and B′ domains make up the cleavage-religation core. Motifs conserved in all topoIIs are shown above the protein schematic, and residues found to be mutated in this study are shown below. The active site tyrosine (Y) is shown in red. B, structure of the core region, B′ and A′, of human topoisomerase IIβ based on the crystal structure of the *S. cerevisiae* topoII core (Berger et al., 1996). Mutated residues selected in this study are shown in green and are labeled. The conserved aspartates of the metal binding site are shown in magenta, and the active site tyrosine is shown in brown.

those affecting the general enzyme mechanism. We report for the first time the selection of mutations with DACA and the use of WAVE to identify mutations. It is interesting that three mutations were selected multiple times with both DACA and AMCA but not with mAMSA and mAMCA. This suggests differences in the ternary complexes of the drug with enzyme and DNA and implicates a role for the acridine methoxy substituent in the selection of drug resistant mutations.

Acknowledgments

We acknowledge Margaret Bell for technical assistance.

References

Austin CA and Marsh KL (1998) Eukaryotic DNA topoisomerase IIβ. *Bioessays* **20:**215–226.

Austin CA, Marsh KL, Wasserman RA, Willmore E, Sayer PJ, Wang JC, and Fisher LM (1995) Expression, domain structure, and enzymatic properties of an active recombinant human DNA topoisomerase IIβ. *J Biol Chem* **270:**15739–15746.

Baguley BC, Leteurtre F, Riou J-F, Finlay GJ, and Pommier Y (1997) A carbamate analogue of amsacrine with activity against non-cycling cells stimulates topoisomerase II cleavage at DNA sites distinct from those of amsacrine. *Eur J Cancer* **33:**272–279.

Beese LR and Steitz TA (1991) Structural basis for the 3′-5′ exonuclease activity of *Escherichia coli* DNA polymerase I: a two metal ion mechanism. *EMBO (Eur Mol Biol Organ) J* **10:**25–33.

Berger JM, Gamblin SJ, Harrison SC, and Wang JC (1996) Structure and mechanism of DNA topoisomerase II. *Nature (Lond)* **379:**225–232.

Capranico G, Guano F, Moro S, Zagotto G, Sissi C, Gatto B, Zunino F, Menta E, and Palumbo M (1998) Mapping drug interactions at the covalent topoisomerase II-DNA complex by bisantrene/amsacrine congeners. *J Biol Chem* **273:**12732–12739.

Errington F, Willmore E, Leontiou C, Tilby MJ, and Austin CA (2004) Differences in the longevity of topoIIα and topoIIβ drug-stabilised cleavable complexes and the relationship to drug sensitivity. *Cancer Chemother Pharmacol* **53:**155–162.

Errington F, Willmore E, Tilby MJ, Li L, Li G, Li W, Baguley BC, and Austin CA (1999) Murine transgenic cells lacking DNA topoisomerase IIβ are resistant to acridines and mitoxantrone: analysis of cytotoxicity and cleavable complex formation. *Mol Pharmacol* **56:**1309–1316.

Finlay GJ, Riou JF, and Baguley BC (1996) From Amsacrine to DACA (N-[2-(Dimethylamino)ethyl]acridine-4-carboxamide): selectivity fro topoisomerases I and II among acridine derivatives. *Eur J Cancer* **32A:**708–714.

Fisher LM, Lawrence JM, Josty IC, Hopewell R, Margerrison EE, and Cullen ME (1989) Ciprofloxacin and the fluoroquinolones. New concepts on the mechanism of action and resistance. *Am J Med* **87:**2S–8S.

Gilroy KL, Leontiou C, Padget K, Lakey JH, and Austin CA (2006) mAMSA resistant human topoisomerase IIβ mutation G465D has reduced ATP hydrolysis activity. *Nucleic Acids Res* **34:**1597–1607.

Hinds M, Deisseroth K, Mayes J, Altschuler E, Jansen R, Ledley FD, and Zwelling LA (1991) Identification of a point mutation in the topoisomerase II gene from a human leukaemia cell line containing an amsacrine-resistant form of topoisomerase II. *Cancer Res* **51:**4729–4731.

Huff AC and Kreuzer KN (1990) Evidence for a common mechanism of action for antitumor and antibacterial agents that inhibit type II DNA topoisomerases. *J Biol Chem* **265:**20496–20505.

Jehn U (1989) New drugs in the treatment of acute and chronic leukaemia: current role of mAMSA. *Bone Marrow Transplant* **4 (Suppl 3):**53–58.

Jensen LH, Wessel I, Moller M, Nitiss JL, Sehested M, and Jensen PB (2000) N-terminal and core-domain random mutations in human topoisomerase II alpha conferring bisdioxopiperzine resistance. *FEBS Lett* **480:**201–207.

Lee M-S, Wang JC, and Beran M (1992) Two independent amsacrine-resistant human myeloid leukemia cell lines share an identical point mutation on the 170 kDa form of human topoisomerase II. *J Mol Biol* **223:**837–843.

Leontiou C, Lakey JH, and Austin CA (2004) Mutation E522K in human DNA topoisomerase IIβ confers resistance to methyl *N*-(4′-(9-acridinylamino)-phenyl)carbamate hydrochloride and methyl *N*-(4′-(9-acridinylamino)-3-methoxyphenyl) methane sulphonamide but hypersensitivity to etoposide. *Mol Pharmacol* **66:**430–439.

Leontiou C, Lakey JH, Lightowlers R, Turnbull RM, and Austin CA (2006) Mutation P732L in human DNA topoisomerase IIβ abolishes DNA cleavage in the presence of calcium and confers drug resistance. *Mol Pharmacol* **69:**130–139.

Leontiou C, Lightowlers R, Lakey JH, and Austin CA (2003) Kinetic analysis of human topoisomerase IIalpha and beta DNA binding by surface plasmon resonance. *FEBS Lett* **554:**206–210.

Marsh KL, Willmore E, Tinelli S, Cornarotti M, Meczes EL, Capranico G, Fisher LM, and Austin CA (1996) Amsacrine-promoted DNA cleavage site determinants for the two human DNA topoisomerase II isoforms α and β. *Biochem Pharmacol* **52:**1675–1685.

Meczes EL, Marsh KL, Fisher LM, Roger MP, and Austin CA (1997) Complementation of temperature-sensitive topoisomerase II mutations in *Saccharomyces cerevisiae* by a human TOP2 beta construct allows the study of topoisomerase II beta inhibitors in yeast. *Cancer Chemother Pharmacol* **39:**367–375.

Moreland N, Finlay GJ, Dragunow M, Holdaway KM, and Baguley BC (1997) Cellular responses to methyl-*N*-[4-(9-acridinylamino)-2-methoxy[henyl]carbamate hydrochloride, an analogue of amsacrinective against non-proliferating cells. *Eur J Cancer* **33:**1668–1676.

Nitiss JL (1994) Using yeast to study resistance to topoisomerase II-targeting drugs. *Cancer Chemother Pharmacol* **34 (Suppl):**S6–S13.

Noble CG and Maxwell A (2002) The role of GyrB in the DNA cleavage-religation reaction of DNA gyrase: a proposed two metal-ion mechanism. *J Mol Biol* **318:**361–371.

Padget K, Pearson AD, and Austin CA (2000) Quantitation of DNA topoisomerase II alpha and beta in human leukaemia cells by immunoblotting. *Leukemia* **14:**1997–2005.

Pan X-S, Ambler J, Mehtar S, and Fisher LM (1996) Involvement of topoisomerase IV and DNA gyrase as ciprofloxacin targets in *Streptococcus pneumoniae*. *Antimicrob Agents Chemother* **40:**2321–2326.

Patel S, Keller BA, and Fisher LM (2000) Mutations at Arg486 and Glu571 in Human Topoisomerase IIα Confer Resistance to Amsacrine: Relevance for Antitumor Drug Resistance in Human Cells. *Mol Pharmacol* **57:**784–791.

Pommier Y (1993) DNA topoisomerase I and II in cancer chemotherapy: update and perspectives. *Cancer Chemother Pharmacol* **32:**103–108.

Turnbull RM, Meczes EL, Perenna Rogers M, Lock RB, Sullivan DM, Finlay GJ, Baguley BC, and Austin CA (1999) Carbamate analogues of amsacrine active against non-cycling cells: relative activity against topoisomerases IIα and β. *Cancer Chemother Pharmacol* **44:**275–282.

Wasserman R and Wang JC (1994) Analysis of yeast DNA topoisomerase II mutants resistant to the antitumor drug amsacrine. *Cancer Res* **54:**1795–1800.

West KL, Meczes EL, Thorn R, Turnbull RM, Marshall R, and Austin CA (2000) Mutagenesis of E477 or K505 in the B′ domain of human topoisomerase II beta increases the requirement for magnesium ions during strand passage. *Biochemistry* **39:**1223–1233.

Willmore E, Frank AJ, Padget K, Tilby MJ, and Austin CA (1998) Etoposide targets topoisomerase IIalpha and IIbeta in leukemic cells: isoform—specific cleavable complexes visualized and quantified in situ by a novel immunofluorescence technique. *Mol Pharmacol* **54:**78–85.

Wulfert M, Tapprich C, and Gattermann N (2006) Optimized PCR fragments for heteroduplex analysis of the whole human mitochondrial genome with denaturing HPLC. *J Chromatogr B* **831:**236–247.

Address correspondence to: Dr. Caroline A. Austin, The Institute for Cell and Molecular Biosciences, The Medical School, Newcastle University, Framlington Place, Newcastle Upon Tyne, NE2 4HH, United Kingdom. E-mail: caroline.austin@ncl.ac.uk